

A Discrete Nonlinear Model with Substrate Feedback

P. G. Kevrekidis^{1,2}, B. A. Malomed^{2,3} and A. R. Bishop²¹ Department of Mathematics and Statistics, University of Massachusetts, Amherst, MA 01003-4515, USA² Center for NonLinear Studies and Theoretical Division, MS B 258, Los Alamos National Laboratory, Los Alamos, NM 87545, USA³ Department of Interdisciplinary Studies, Faculty of Engineering, Tel Aviv University, Tel Aviv 69978, Israel
(October 26, 2021)

We consider a prototypical model in which a nonlinear field (continuum or discrete) evolves on a flexible substrate which feeds back to the evolution of the main field. We identify the underlying physics and potential applications of such a model and examine its simplest one-dimensional Hamiltonian form, which turns out to be a modified Frenkel-Kontorova model coupled to an extra linear equation. We find static kink solutions and study their stability, and then examine moving kinks (the continuum limit of the model is studied too). We observe how the substrate effectively renormalizes properties of the kinks. In particular, a nontrivial finding is that branches of stable and unstable kink solutions may be extended beyond a critical point at which an effective intersite coupling vanishes; passing this critical point does not destabilize the kink. Kink-antikink collisions are also studied, demonstrating alternation between merger and transmission cases.

I. INTRODUCTION

Soft condensed matter systems, such as vesicles, microtubules and membranes, have recently attracted a lot of attention in both biological and industrial applications [1,4]. More generally, physical systems at the nanoscale including nanotubes and electronic and photonic waveguide structures [5,6] have nontrivial geometry and are influenced by substrate effects. These wide classes of problems, many of which are inherently nonlinear, raise the question of the interplay between nonlinearity and an adaptive substrate, including, in particular, a possibility of developing curvature in the substrate due to feedback forces from the nonlinear system. Some of these systems such as, for instance, the DNA double strand [7,8], are also inherently discrete.

In this situation, the derivation of evolutionary equations for intrinsic fields in a nonlinear system interfacing with a flexible substrate should take into regard the local dynamics and the feedback of the substrate. A context where these phenomena can easily manifest themselves is elasticity. Usually, models of particles connected by springs, such as the Frenkel-Kontorova (FK) model [9], assume that the springs are strictly linear. However, in reality the spring constant may depend on the spring's stretch. In this case, we are meaning not a straightforward generalization of the FK model that includes the spring's anharmonicity, but a different system, in which the spring constant obeys its own dynamical equation, see below.

There is an increasing body of literature dealing with the interplay of nonlinearity, discreteness, and a substrate subject to curvature. Usually, even if the substrate is curved, its geometry is assumed to be fixed, see, e.g., Refs. [10]. However, for many applications, ranging from condensed matter to optics to biophysics, it is quite relevant

to examine a prototypical model that admits a possibility of a variable substrate, which is affected by the primary field(s) and feeds back into its (their) dynamics.

In this work, we introduce a simple one-dimensional model which captures some of the physically essential features of the interplay of a nonlinear system with a flexible substrate. A natural setting for the model is a lattice with on-site nonlinearity, or its continuum counterpart (see below), hence the first ingredient of the system is the FK model (alias the discrete sine-Gordon equation [11]):

$$u_n = C \nabla^2 u_n - \sin u_n; \quad (1)$$

where C is the coupling constant (the spring constant, if we consider adjacent sites as being coupled by springs), $\nabla^2 u_n = (u_{n+1} + u_{n-1} - 2u_n)$ is the discrete Laplacian, while the last term in Eq. (1) is the on-site nonlinearity. The overdot denotes the temporal derivative, while n indexes the lattice sites. The FK model has a plethora of physical realizations, the simplest one being the Scott's model, i.e., a chain of pendula suspended on a torque-elastic thread [12].

The springs can be made nonlinear by assuming that the constant C in Eq. (1) is replaced by a site-dependent one, $C_n = C_0 + v_n$, where C_0 is the constant mean value, while v_n is the variation of the spring constant due to the variation of the displacements u_n and u_{n-1} at the sites that the spring couples. The simplest nontrivial possibility, provided that we aim to produce a Hamiltonian system, is to assume that v_n responds to a change in displacements according to the following equation:

$$v_n = -[\gamma (u_n - u_{n-1})]; \quad (2)$$

where γ is an intrinsic stiffness of the spring (see below), and k accounts for its susceptibility to the stretch. We

use the convention (see also a sketch of the system in Fig. 1) that the n -th spring connects the sites $n-1$ and n . To maintain the Hamiltonian character and self-consistency of the model, the equation for the field u_n should be modified [cf. Eq. (1)] to read:

$$u_n = C_0 - 2u_n \sin u_n + k(v_n - v_{n+1}); \quad (3)$$

In fact, the extra term added to Eq. (3) can be easily understood in terms of the mechanical model: a difference in the value of the string constant produces a difference in the elastic forces even if there is no change in the length of the springs. Equations (2) and (3) are derived from the Hamiltonian

$$H = \sum_n \left[\frac{1}{2} u_n^2 + \frac{v_n^2}{2} + \frac{1}{2} v_n^2 + (1 - \cos(u_n)) \right] + \frac{C_0}{2} (u_n - u_{n-1})^2 - k v_n (u_n - u_{n-1});$$

We note that a somewhat similar (but still significantly different) two-component model was proposed to describe the coupling between protons and heavy ions in Ref. [13] (see also references therein). A single-component model with nonlinear springs was examined (mainly in terms of its thermodynamic properties) in Ref. [14].

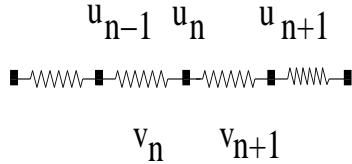


FIG. 1. Sketch of the model. v_n is the deviation of the n -th spring constant from C_0 due to the discrete gradient of the displacement u_n .

While this work is focused on the simplest model based on Eqs. (2) and (3), which includes only the linear coupling between the fields u_n and v_n , we note that a relevant generalization may involve quadratic couplings:

$$u_n = C_0 - 2u_n \sin(u_n) + k(v_n - v_{n+1}) + r v_n (u_{n-1} - u_n) + r v_{n+1} (u_{n+1} - u_n); \quad (4)$$

$$v_n = -k(u_n - u_{n-1}) - \frac{r}{2}(u_n - u_{n-1})^2; \quad (5)$$

The origin of the quadratic terms is evident: they stem from second-order effects combining the change in the string length and elasticity.

The continuum limit (CL) of Eqs. (4) and (5) is

$$u_{tt} = u_{xx} \sin u - k v_x + r(v u_x)_x; \quad (6)$$

$$v_{tt} = -v + k u_x + \frac{r}{2} u_x^2; \quad (7)$$

where the constants k and r were appropriately rescaled, and the subscripts stand for partial derivatives. Setting $r = 0$ in Eqs. (6) and (7) yields the CL of Eqs. (2) and (3). Note that, even in the latter case, the Lorentz invariance of the CL equations is broken (in comparison with the sine-Gordon equation, which is the CL of the usual FK model). An exact solution for the static kink (the topological soliton in the u subsystem) can be easily found (for the case $r = 0$; is then rescaled to be 1),

$$u = 4 \tan^{-1} \exp \left[\frac{x - x_0}{1 - k^2} \right]; \quad (8)$$

$$v = 2 \frac{k}{1 - k^2} \operatorname{sech} \left[\frac{x - x_0}{1 - k^2} \right]; \quad (9)$$

but exact solutions for moving kinks are not available even in the CL limit.

Also worth noting is the CL for the linear spectrum of extended waves, which can be obtained by substituting $u = A \exp(i(Kx - \omega t))$ and $v = B \exp(i(Kx - \omega t))$ in the linearized version of Eqs. (6) and (7). For $r = 0$ and with the normalization $A = 1$, we obtain

$$\omega^2 = \frac{r}{1 + \frac{1}{2} K^2} \frac{K^2}{K^2 + 4k^2};$$

which consists of two phonon bands, one with $\omega^2 < 1$, and the other one with $\omega^2 > 1$. Notice the presence of a finite gap between these bands, provided that $k \neq 0$. In the case $|k| = 1$, the lower branch of the linearized spectrum is acoustic, while the upper one is always of the optical (alias, plasmon) type.

Returning to the discrete case, there is no explicit solution for the static case; however, after the substitution of $v_n = (k=) (u_n - u_{n-1})$, which follows from Eq. (3), the steady-state equation for u_n becomes

$$(C_0 - k^2 =) - 2u_n = \sin u_n; \quad (10)$$

and hence k effectively renormalizes the lattice coupling. In fact that is what can be observed from Eqs. (8) and (9), as well as from Fig. 2: the effect of k is to decrease the width of the kink (by a factor approximately equal to $|k|$ for k small). As is well known [11,15], a narrower kink is less mobile. A numerical solution of the static discrete equation (10) yields, similar to the case of the regular FK model [11,15], two types of steady-state discrete kinks, namely a stable inter-site centered one (an example for $C_0 = 2k = 1$ is shown in Fig. 2) and an unstable site-centered one.

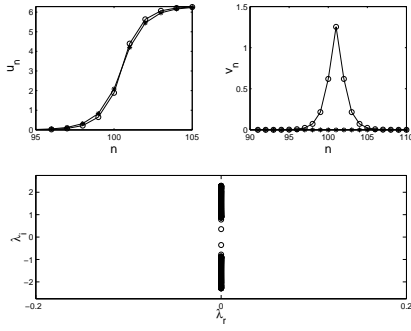


FIG. 2. A stable static intersite-centered kink (u_n and v_n components are shown by circles in the top left and top right plots, respectively) for $C_0 = 1$ and $k = 0.5$; solid lines connecting circles are guides to the eye. For comparison, the fields are also shown for the case $k = 0$, which corresponds to the usual FK model (stars connected by solid lines). The bottom subplot shows the spectral plane (λ_r ; λ_i) of linear stability eigenvalues found from the linearization of Eqs. (2) and (3) around the kink (for $k = 0.5$; the subscripts i and r refer to the real and imaginary parts of the eigenvalues). The absence of eigenvalues with nonzero real part implies the stability of the kink. Here, $\lambda_i = 1$.

We have examined the variation of the static kink solutions and of their linear stability eigenvalues (for small perturbations) as a function of $|k|$. Typical examples are shown in Fig. 3 for the stable and unstable kinks for $C_0 = 1$. A surprising finding in both cases is that the solutions could be continued for some range beyond the point $|k| = 1$, which is effectively equivalent to the zero-coupling (anti-continuum) limit, see Eq. (10). The shape of the solutions found for $|k| > 1$ is non-monotonic (but they remain stable). These solution branches terminate at $|k| = 1.04$ for the stable solution, and at $|k| = 1.07$ for the unstable site-centered one.

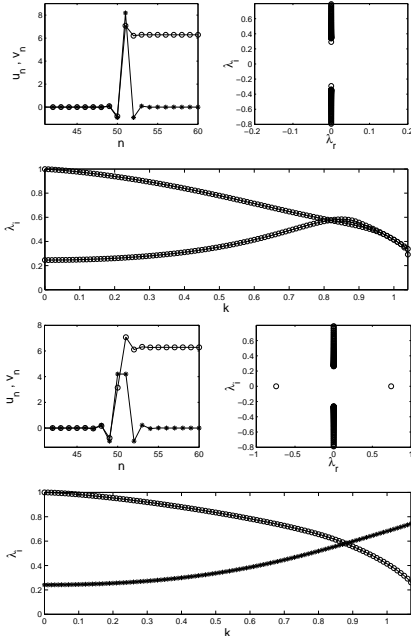


FIG. 3. The top subplot shows the intersite-centered solution and its stability (top left and right panels) for $|k| = 1.04$ (just prior to the branch termination). The bottom panel shows the two stable internal mode eigenvalues of the intersite-centered kink (circles connected by the solid line) vs. k . The bottom subplots show the same for the unstable site-centered solution (the two top panels are for $k = 1.07$, i.e., also just prior to the termination of the corresponding branch, and the stars in the bottom subplot show the unstable eigenvalue). Note that the profiles of both kinks are non-monotonic.

The above-mentioned expectation that the kink becomes less mobile as $|k|$ increases is verified dynamically by taking an initial kink boosted to the speed $c = 0.2$. Solving Eqs. (6) and (7) (with $r = 0$) with this initial condition for different values of k , we notice that, as is shown in Fig. 4, the kink travels farther for $k = 0$ than it does for $k \neq 0$, despite the fact that the initial velocity is the same in all the cases. In other words, the effective velocity which the kink demonstrates differs from that which was lent to it initially, and it also depends on $|k|$.

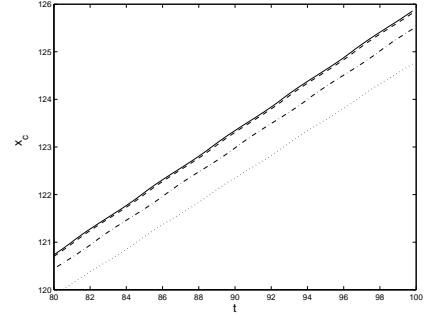


FIG. 4. Trajectories of a continuum-limit kink, initially boosted to the velocity $c = 0.2$, obtained from the numerical integration of Eqs. (2) and (3) at different values of k . $k = 0$; $k = 0.05$; $k = 0.15$, and $k = 0.25$ correspond, respectively, to the solid, dashed, dash-dotted, and dotted lines. The trajectories are shown only for late stage of the time evolution.

Finally, we have also examined kink-antikink collisions in the system of Eqs. (2) and (3). An example of this type is shown in Fig. 5. In this case, $C_0 = 16/9$ ($\hbar = 0.75$), and the initial speeds of the kink and antikink are 0.1 . The figure indicates the possibility of existence of parameter windows for which the kinks eventually escape each other's attraction (upon multiple bounces). Such windows lie between intervals of merger (kink-antikink annihilation into a breather). This feature is reminiscent of well-known findings of Ref. [16] for kink-antikink collisions in continuum (nonintegrable) models. However, unlike what was found in that work, here the windows are in terms of the parameter k , observed at a fixed value of the collision velocity.

An example of such a window (a characteristic case of which is shown in Fig. 5) occurs for $0.176 \leq k \leq 0.179$, even though in the FK model (e.g., for $k = 0$, a case

also shown in Fig. 5), for $v = 0.1$, only annihilation is possible. Notice that for this value (0.1) of the initial speed (and within our resolution steps of 0.001 in k), no additional windows were identified. However, by considering different values of the initial speed (such as e.g., $v = 0.125$), we have verified that typically multiple such windows can occur. The dynamical behavior of the present model, which is essentially richer than in its FK counterpart, is provided for by the fact that the kink's internal mode is affected by variations of the coupling to the substrate (see the discussion above).

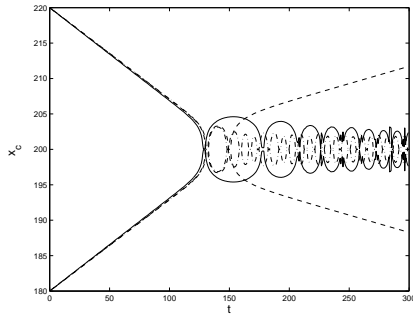


FIG. 5. Kink-antikink collisions for $C_0 = 16/9$ ($\hbar = 0.75$) and initial speeds 0.1 are shown in terms of trajectories of centers of the colliding kinks. The solid, dashed and dash-dotted lines correspond, respectively, to $k = 0.0$, $k = 0.178$ and $k = 0.2$.

The case of $\omega = 0$ in Eq. (2) has its own interest, as in this case v_n may be regarded as an acoustic phonon branch (the one without a gap in its dispersion relation), which interacts with the optical (plasmon) branch represented by the field u_n . Equations (2) and (3) with $\omega = 0$ furnish an elementary example of this type of interaction. In this case, the equations have solely uniform zero-velocity solutions. Nontrivial solutions may only exist with a finite speed c . In particular, the model's CL gives rise, in this case, to a double (4) kink (not shown here), which is produced by the equation $(1 - c^2)u'' = \sin(u) + (k^2 - c^2)u = 0$, where $x = ct$. However, this simplest version of the model with $\omega = 0$ is flawed, as its Hamiltonian is unbounded from below, hence the model is not a well-posed one. It can be amended to fix this problem, keeping the optical-phonon and acoustic-phonon character of the fields u_n and v_n , but detailed consideration of this issue is beyond the scope of the present work.

To conclude, in this work we have proposed a simple, prototypical model, that may be developed to describe dynamics of kink-shaped excitations in more complex systems. A noteworthy extension would be the gener-

alization of the model to two dimensions, which may be very relevant for physical applications. Furthermore, dissipative versions of the model can be of direct relevance to chemical and biophysical applications. Detailed consideration of higher-order feedback effects, collisions between kinks, and long-lived breather-like states in this model would also be of interest.

This research was supported by the US Department of Energy under the contract W-7405-ENG-36.

-
- [1] E. Sackmann, in R. Lipowsky and E. Sackmann (Eds.), *The Structure and Dynamics of Membranes: Handbook of Biological Physics*, vol. 1 (Elsevier, Amsterdam, 1995).
 - [2] U. Seifert, *Adv. in Phys.* 46, 13 (1997).
 - [3] W. Saenger, *Principles of Nucleic Acid Structure* (Springer-Verlag: Berlin, 1984).
 - [4] *Physics of Amphiphilic Layers*. J. Meunier, D. Langevin, and D. Boccardo (Eds.) (Springer-Verlag: Berlin, 1997).
 - [5] Y. Imry, *Introduction to Mesoscopic Physics* (Oxford University Press: New York, 1997).
 - [6] *Photonic Band Gaps and Localization*. C.M. Soukoulis (Ed.) (Plenum Press: New York, 1993).
 - [7] C. Reiss, in *Nonlinear Excitations in Biomolecules*, M. Peyrard (Ed.) (Springer-Verlag: Berlin, 1995), p. 29.
 - [8] M. Peyrard and A.R. Bishop, *Phys. Rev. Lett.* 62, 2755 (1989).
 - [9] J. Frenkel and T. Kontorova, *J. Phys. USSR* 1, 137 (1939).
 - [10] See e.g., Yu. B. Gaididei, S. F. Mingaleev, and P. L. Christiansen, *Phys. Rev. E* 62, R53 (2000); M. Ibanes, J. M. Sancho, and G. P. Tsironis, *Phys. Rev. E* 65, 041902 (2002);
 - [11] M. Peyrard and M.D. Kruuskal, *Physica D* 14, 88 (1984); O.M. Braun and Yu.S. Kivshar, *Phys. Rep.* 306, 1 (1998).
 - [12] A.C. Scott, *Am. J. Phys.* 37, 52 (1969).
 - [13] M. Peyrard, St. Pnevmatikos and N. Flytzanis, *Phys. Rev. A* 36, 903 (1987).
 - [14] W.C. Kerr, A.M. Hawthorne, R.J. Gooding, A.R. Bishop and J.A. Krumhansl, *Phys. Rev. B* 45, 7036 (1992).
 - [15] O.M. Braun, Yu.S. Kivshar and M. Peyrard, *Phys. Rev. E* 56, 6050 (1997); N.J. Balmforth, R.V. Craster and P.G. Kevrekidis, *Physica D* 135, 212 (2000); P.G. Kevrekidis and C.K.R.T. Jones, *Phys. Rev. E* 61, 3114 (2000); P.G. Kevrekidis and M.I. Weinstein, *Physica D* 142, 113 (2000).
 - [16] D.K. Campbell, J.F. Schonfeld, and C.A. Wingate, *Physica D* 9, 1 (1983).